Vibrational Energy Flow Rates for *cis*- and *trans*-Stilbene Isomers in Solution

M. Jocelyn Cox and F. Fleming Crim*

Department of Chemistry, University of Wisconsin - Madison, Madison, Wisconsin 53706

Received: August 1, 2005; In Final Form: October 7, 2005

Transient electronic absorption following excitation of the first C−H stretching overtone ($2\nu_{CH}$) or a C−H stretch−bend combination ($\nu_{CH} + \nu_{bend}$) monitors the flow of vibrational energy in *cis*-stilbene and in *trans*-stilbene. Following a rapid initial rise as energy flows into states interrogated by the probe pulse, the absorption decays with two time constants, which are about a factor of 2 longer for the cis-isomer than for the trans-isomer. The decay times for *cis*-stilbene are $\tau_2^{cis} = (2.6 \pm 1.5)$ ps and $\tau_3^{cis} = (24.1 \pm 2.1)$ ps, and those for *trans*-stilbene are $\tau_2^{trans} = (1.4 \pm 0.6)$ ps and $\tau_3^{trans} = (10.2 \pm 1.1)$ ps. The decay times are essentially the same in different solvents, suggesting that the relaxation is primarily *intramolecular*. The two decay times are consistent with the sequential flow of energy through sets of coupled states within the molecule, and the difference in the rates for the two isomers likely reflects differences in coupling among the states arising from the different structures of the isomers. The similarity of the time evolution following excitation of the first C−H overtone at 5990 cm^{-1} and the stretch−bend combination at 4650 cm^{-1} is consistent with a subset of states, whose structure is similar for the two vibrational excitation energies, controlling the observed flow of energy.

I. Introduction

The importance of vibrations in the evolution of a reactive system makes the flow of energy within a molecule and from a molecule into its surroundings essential in chemistry. The flow of energy within a molecule, intramolecular vibrational relaxation (IVR), distributes energy at a rate that depends on the couplings between the initially excited state and each of the energetically accessible states. The transfer of energy into the surroundings, intermolecular energy transfer (IET), moves energy from the initially excited molecule into other molecules. In solution, this process corresponds to the flow of energy from the solute into vibrations of the solvent molecules as well as into collective modes of the solvent. Thus, it depends both on the vibrational modes of the solute and on the solvent environment. Some modes transfer energy to the solvent more efficiently than others, and generally, vibrational energy flows within a molecule until it reaches such a mode, which in turn efficiently transfers energy into the solvent.

One goal of vibrational relaxation studies is to identify the features that control the rate of energy flow,[1−3] and experiments have used chemical substitutions[4−9] to reveal systematic changes in vibrational relaxation rates. Relatively small structural changes can alter the energies of the vibrations and their coupling to each other and, thus, influence the pathways of energy flow within a molecule and into the solvent. Geometric isomers offer a useful approach to examining the mechanism of energy transfer because their vibrational state structure and coupling differ even though their chemical composition is the same. Our goal here is to determine the vibrational relaxation rate and mechanism in the cis- and trans-isomers of stilbene.

Gas-phase studies show that the IVR rates in a pair of conformers can differ by orders of magnitude. High-resolution spectroscopy of conformational isomers stabilized at low temperature in molecular beams has determined the energies and widths of transitions to molecular eigenstates, the analysis of which reveals the anharmonic couplings that govern the flow of energy in isolated molecules. For example, the IVR rates for the conformers of 1-pentyne differ by a factor of two[10] while those for the conformers of allyl fluoride differ by an order of magnitude.[11] In these examples, the two conformers distinguished by rotation around a single bond have different symmetry and, therefore, different numbers of states available for efficient energy transfer. We study vibrational relaxation of the geometric isomers of stilbene in solution by using transient electronic absorption spectroscopy to probe states of the cis- and trans-isomers following initial excitation of two quanta of a C−H stretching vibration.[5] As the initially excited nonstationary state evolves, vibrational energy flows from the C−H stretch into other degrees of freedom, which include Franck−Condon active vibrational modes. Population in these modes enhances the absorption in the long wavelength portion of the $S_1 \leftarrow S_0$ electronic transition, and we follow the flow of vibrational energy through the Franck−Condon active modes by monitoring the changes in the transient electronic absorption.

II. Experimental Approach

The tunable IR excitation and ultraviolet probe pulses come from nonlinear frequency conversion of light from an amplified Ti:sapphire laser. The amplifier produces 1-mJ, 100-fs pulses centered at 800 nm at a repetition rate of 1 kHz. An optical parametric amplifier (OPA) converts about 40% of the 800-nm light into 30 μJ of 1.7-μm (6000 cm^{-1}) light for the vibrational excitation pulse. We frequency double about 90% of the remaining light and pump a noncollinear optical parametric amplifier (NOPA)[12−14] based on a 1-mm type I, β-barium borate (BBO) crystal cut at $\theta = 29°$. Mixing the light from the NOPA with residual 800-nm light in a type I BBO crystal (300 μm, $\theta = 29°$) produces tunable probe light between 290 and 380 nm. A computer-controlled translation stage sets the delay between

* To whom correspondence should be addressed. E-mail: fcrim@chem.wisc.edu.

10.1021/jp054263x CCC: $30.25
Published on Web 11/25/2005

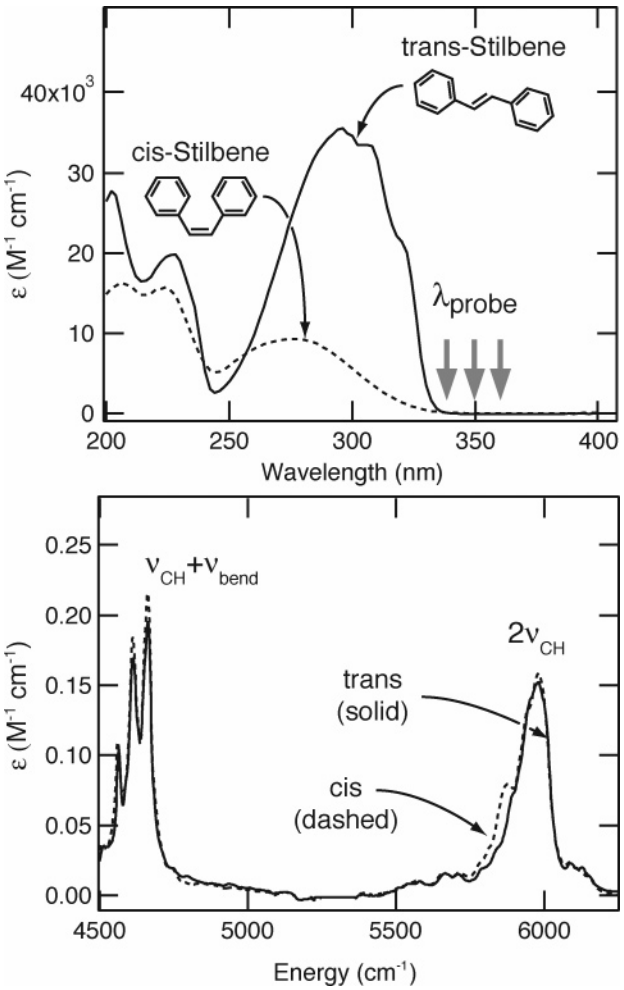

Figure 1. Ultraviolet (upper panel) and near-IR spectra (lower panel) of *cis*- and *trans*-stilbene. The dashed lines show the *cis*-stilbene spectra, and the solid lines show the *trans*-stilbene spectra. The vertical arrows in the upper panel mark the probe wavelengths for the transient absorption measurements.

the pump and probe pulses, and an optical chopper blocks every other pump pulse for active background subtraction. The sample circulates through a flow cell that has a 1-mm path length and 2-mm quartz windows and in which the beams intersect at a small angle. Lenses of 400-mm and 300-mm focal length focus the IR and ultraviolet beams, respectively, into the sample. Attenuating the probe pulse before the sample minimizes photoisomerization, and averaging the signal from between 5000 and 10 000 laser pulses at each delay produces a noise level of 0.1 mOD for *cis*-stilbene and 0.05 mOD for *trans*-stilbene. All reagents and solvents come from commercial sources.

The top portion of Figure 1 shows the electronic absorption spectra of *cis*- and *trans*-stilbene as dashed and solid lines, respectively, and the vertical arrows mark the probe wavelengths we use. There is a weak vibrational progression in the *trans*-stilbene spectrum that is absent in the *cis*-stilbene spectrum, and the maximum of the long wavelength transition lies at a slightly lower energy in the trans-isomer. Because we probe on the long wavelength side of the spectrum, the structured part of the *trans*-stilbene spectrum does not contribute to the signal. As the lower portion of the figure shows, the vibrational spectra in the region of the stretch overtone and the stretch−bend combination band are very similar in *cis*-stilbene (dashed line) and *trans*-stilbene (solid line). Both isomers have 12 C−H stretching vibrations whose energies lie within 60 cm^{-1} of each other,[15] and the transitions to these modes in the first overtone

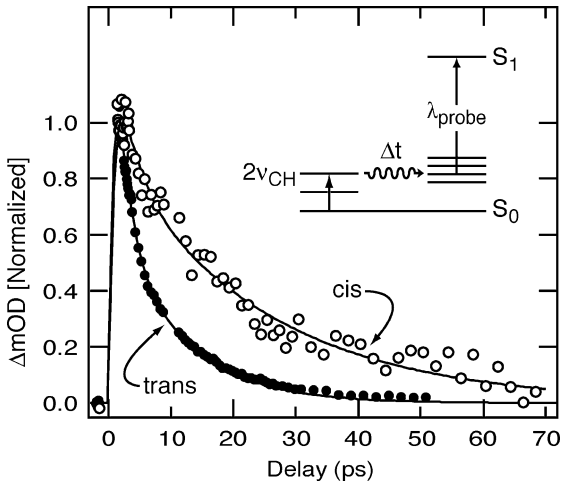

Figure 2. Transient absorption of *cis*-stilbene (open points) and *trans*-stilbene (solid points) following excitation of the first C−H stretching overtone ($2\nu_{CH}$). The probe wavelength is $\lambda_{probe} = 342$ nm, and the solvent is $CDCl_3$. The solid lines are fits of three exponentials to the data that yield the time constants described in the text and given in Table 1. The two decay times for *cis*-stilbene ($\tau_2^{cis} = (2.6 \pm 1.5)$ ps and $\tau_3^{cis} = (24.1 \pm 2.1)$ ps) are about twice those for *trans*-stilbene ($\tau_2^{trans} = (1.4 \pm 0.6)$ ps and $\tau_3^{trans} = (10.2 \pm 1.1)$ ps).

region fall within the 150 cm^{-1} bandwidth of the vibrational excitation laser. Because all of the eigenstates that contain C−H stretching character lie within the excitation bandwidth, we initially prepare a coherent superposition corresponding to two quanta of C−H stretching excitation, but we cannot identify individually excited C−H stretches. The situation is similar for the stretch−bend combination bands, but their transitions lie at the far edge of the tuning range of our OPA, which limits the signals we obtain for those transitions.

III. Results

The temporal evolution of the transient electronic absorption shown in Figure 2 reflects the flow of vibrational energy following excitation of the first overtone of the C−H stretch of *cis*-stilbene (open points) and *trans*-stilbene (closed points) at 5990 cm^{-1}. The energy level diagram in the figure shows the essential features of the experiment. One pulse excites two quanta of C−H stretch, and a second ultraviolet pulse probes intermediate states populated as energy flows through the molecule and into the solvent. The key to monitoring the energy transfer is that many of the states into which energy flows have better Franck−Condon factors for the electronic transition than the initially prepared C−H stretching state. The absorption signal rises as vibrational energy flows from the initially excited C−H stretch overtone into states with good Franck−Condon factors and then decays as it enters modes that have poor Franck−Condon factors.

We fit the transient absorption signal to the sum of three exponentials with time constants τ_1, τ_2, and τ_3 in order to extract times for the rise and decay. A sequential relaxation from the initially excited state, $|2\nu_{CH}\rangle$, through intermediate sets of states, $\{|n_1\rangle\}$ and $\{|n_2\rangle\}$, and then into a set of final states, $\{|g\rangle\}$

$$|2\nu_{CH}\rangle \xrightarrow{\tau_1} \{|n_1\rangle\} \xrightarrow{\tau_2} \{|n_2\rangle\} \xrightarrow{\tau_3} \{|g\rangle\}$$

is consistent with the observed rise and decay. In this scheme, the initial state $|2\nu_{CH}\rangle$ and final states $\{|g\rangle\}$ have small Franck−Condon factors for the $S_1 \leftarrow S_0$ probe transition, and the intermediate states, $\{|n_1\rangle\}$ and $\{|n_2\rangle\}$, have better Franck−

Condon factors. The intermediate states must also have *different* Franck−Condon factors, otherwise the signal would not change as the population moved from one set to another. The simpler approach of fitting the signal with a single rise and single decay does not give even a qualitatively correct fit to the data. The final set of states, $\{|g\rangle\}$, potentially includes states of the stilbene molecule as well as solvent states. As described below, our analysis suggests that energy flow within the molecule dominates the decay of the signal.

The coherent response of the sample when the excitation and probe pulses overlap in time produces a signal, even in the absence of solute molecules, that obscures the fast initial rise of the transient absorption signal. We fit the data only at times greater than 2 ps in order to avoid contributions from this signal and fix the time constant for the initial rise (τ_1) at 1 ps for both *cis*- and *trans*-stilbene. The time constants for the rise (τ_1) and fast component of the decay (τ_2) are strongly coupled, and a range of combinations of the two produce comparable fits. For example, increasing τ_1 from 0.5 to 2 ps for *trans*-stilbene decreases τ_2 from 2.7 to 0.7 ps. Use of the same value of τ_1 for both *cis*- and *trans*-stilbene gives an initial decay time (τ_2) that is about a factor of 2 *larger* in *cis*-stilbene than in *trans*-stilbene. Similarly, fits using the same values of τ_2 for the two isomers give a rise time (τ_1) that is about a factor of 2 larger in *cis*-stilbene than in *trans*-stilbene. The model given below suggests that the rise times are more likely to be the same than the initial decay times, and we make that assumption in our analysis. In addition, fits to a double-exponential decay without any rise find an initial decay that is factor of 2 longer in *cis*-stilbene than in *trans*-stilbene. None of the possible choices of the rise and fast decay time constants influence the time constant (τ_3) for the slow decay.

Our fit of the signal, $S(t)$, uses the sequential kinetics scheme shown above with adjustable amplitudes for $\{|n_1\rangle\}$ and $\{|n_2\rangle\}$, reflecting their different Franck−Condon factors. Thus, the signal is $S(t) \propto A_1\Delta P_1 + A_2\Delta P_2$, where ΔP_1 and ΔP_2 are the transient excess populations of $\{|n_1\rangle\}$ and $\{|n_2\rangle\}$ and A_1 and A_2 are adjustable amplitudes. To obtain the most consistent decay constants, we follow a stepwise procedure in which we initially fit the transient signal for an isomer using all four variables (τ_2, τ_3, A_1, and A_2) as free parameters with $\tau_1 = 1$ ps. We then average the resulting fast decay times for each isomer to obtain $\tau_2^{cis} = (2.6 \pm 1.5)$ ps for *cis*-stilbene and $\tau_2^{trans} = (1.4 \pm 0.6)$ ps for *trans*-stilbene. We repeat the fit using these fixed values to obtain the best value of τ_3. The second decay time (τ_3), which does not depend on the values of τ_1 and τ_2, is $\tau_3^{cis} = (24.1 \pm 2.1)$ ps in *cis*-stilbene and $\tau_3^{trans} = (10.2 \pm 1.1)$ ps in *trans*-stilbene. The uncertainties are the range of values given by fits to multiple traces and encompass both the variation among the traces and the statistical uncertainties in fitting each trace. This procedure produces the most reliable values for the slowest decay time. (The quality of the individual fits is comparable to that obtained allowing both τ_2 and τ_3 to vary, but the reproducibility of τ_3 among individual traces is considerably better when we fix τ_2.) The best fit for *trans*-stilbene in $CDCl_3$ gives a ratio of coefficients $A_1/A_2 = 3.4$, which in the context of a sequential kinetics model reflects the larger Franck−Condon factors and, hence, greater absorption probability for the first set of states $\{|n_1\rangle\}$. (Table 1 gives the decay times and amplitudes from the fits.) The fits for different probe wavelengths differ slightly, but the range of wavelengths is too small for us to extract a systematic variation.

There are no direct comparisons for the vibrational relaxation of stilbene at our initial excitation energies of 4500 and 6000 cm^{-1}. Two experiments probing the evolution of vibrational energy at much higher levels in the ground electronic state use internal conversion following ultraviolet excitation to create *trans*-stilbene with more than 30 000 cm^{-1} of internal energy.[16−18] Sension et al. followed the excited-state isomerization of *cis*-stilbene in hexane and used laser-induced fluorescence to observe ground electronic state *trans*-stilbene molecules produced by internal conversion to S_0 following the excitation of *cis*-stilbene to S_1.[16,17] They inferred a vibrational relaxation time of about 10 ps from the narrowing of the fluorescence excitation spectrum as the initially formed vibrationally excited stilbene relaxed. In an experiment using a similar excitation scheme, Nikowa et al. obtained the temporal evolution of *trans*-stilbene from wavelength-dependent fluorescence quantum yields and observed a 1 to 2 ps decay along with a longer 10 ps decay in *n*-pentane and methanol.[18] In both cases, excitation energy is much higher than in our measurements, and energy redistribution during the isomerization and internal conversion makes the initial internal energy distribution more nearly random. The relaxation in these cases must include a large component of transfer to the solvent since there is extensive intramolecular energy transfer prior to the beginning of the relaxation measurement. Experiments observing intramolecular energy flow at relatively low levels of excitation in S_1 using anti-Stokes Raman scattering find IVR times of 3 to 5 ps that are on the same order as we measure in S_0 and lead to the conclusion that IVR in the S_1 state also proceeds in two steps.[19−21]

TABLE 1: Decay Times and Relative Amplitudes for *cis*- and *trans*-Stilbene in Different Solvents

trans-stilbene

solvent	τ_1 (ps)	τ_2 (ps)	τ_3 (ps)	A_1/A_2
first overtone ($2\nu_{CH}$)				
$CDCl_3$	1	1.4 ± 0.6	10.2 ± 1.1	3.4 ± 0.3
$(CD_3)_2CO$	1	1.4 ± 0.6	10.3 ± 1.9	3.6 ± 0.4
CD_3CN	1	1.4 ± 0.6	9.7 ± 1.4	3.2 ± 0.3
combination band ($\nu_{CH} + \nu_{bend}$)				
$CDCl_3$	1	1.2 ± 0.8	8.8 ± 1.8	4.4 ± 1.7

cis-stilbene

solvent	τ_1 (ps)	τ_2 (ps)	τ_3 (ps)	A_1/A_2
first overtone ($2\nu_{CH}$)				
$CDCl_3$	1	2.6 ± 1.5	24.1 ± 2.1	1.8 ± 0.2
$(CD_3)_2CO$	1	2.6 ± 1.5	21.7 ± 2.8	2.5 ± 0.5
combination band ($\nu_{CH} + \nu_{bend}$)				
$CDCl_3$	1	3.2 ± 1.1	22.2 ± 1.2	2.7 ± 0.3

The decay times that we observe are relatively insensitive to both the identity of the solvent and the initial vibrational energy. The 2-fold decrease in relaxation times between the cis- and trans-isomers is larger than any differences from the solvent environment or excitation level. Figure 3 shows the transient electronic absorption of stilbene excited in the region of the first C−H stretching overtone in two different solvents. The upper panel compares the decay of the transient electronic absorption for *trans*-stilbene in deuterated choloroform ($CDCl_3$) and deuterated acetone ($(CD_3)_2CO$). Although the two solvents interact with stilbene differently, the decays of the transient absorption for *trans*-stilbene are almost identical to each other as are those shown in the lower panel for *cis*-stilbene. As Table 1 shows, we also observe nearly the same decay time for *trans*-stilbene in deuterated acetonitrile (CD_3CN). (Limited measurements in CCl_4 give very similar relaxation times as well.) Dispersion forces (and possibly complex formation for acetone and acetonitrile) are the dominant interactions of the

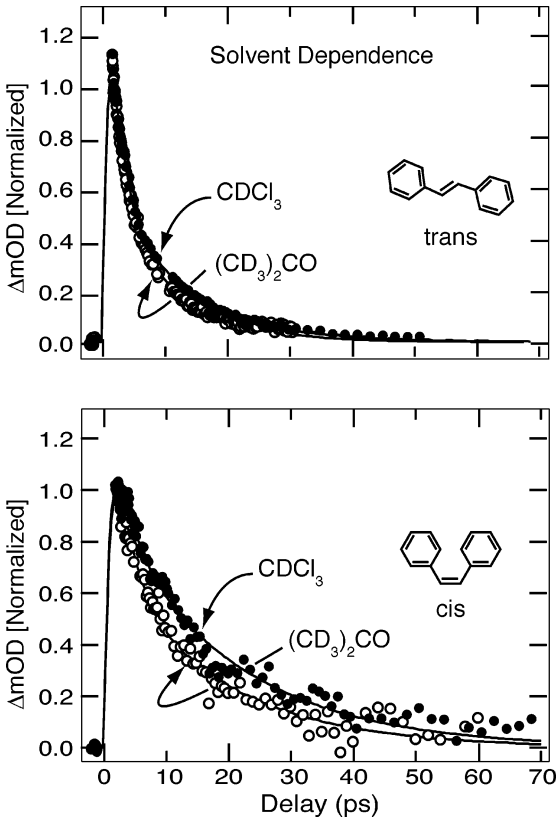

Figure 3. Solvent dependence of the transient absorption of *cis*-stilbene (lower panel) and *trans*-stilbene (upper panel) following excitation of the first C−H stretching overtone ($2\nu_{CH}$) in deutero-chloroform (solid points) and in deutero-acetone (open points). The time evolution is almost identical for the two solvents despite their different interaction strengths.

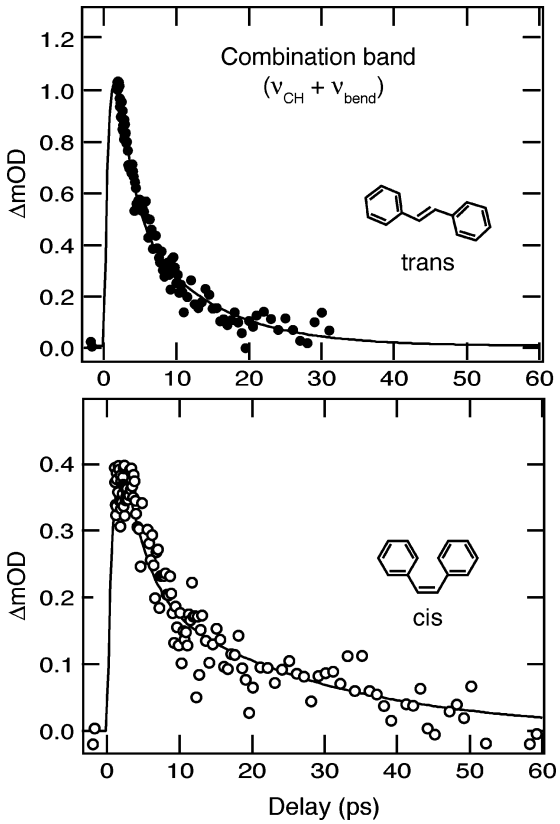

Figure 4. Transient absorption of *cis*-stilbene (open points) and *trans*-stilbene (solid points) following excitation of the stretch−bend combination band ($\nu_{CH} + \nu_{bend}$). The probe wavelength is $\lambda_{probe} = 348$ nm, and the solvent is $CDCl_3$. The solid lines are curves calculated using the decay times obtained from fitting the first overtone.

solvent with stilbene, and the polarizability volumes[22] of the three solvents range from 4.5 Å^3 for CH_3CN to 8.5 Å^3 for $CHCl_3$, giving a variety of interaction strengths. Nonetheless, we observe virtually identical relaxation times in the different solvents.

This relative indifference to the solvent identity suggests that the relaxation is largely an intramolecular process. Comparison of the transient electronic absorption following excitation of the first C−H stretch overtone ($2\nu_{CH}$) and the stretch−bend combination ($\nu_{CH} + \nu_{bend}$) also shows that the time evolution does not depend strongly on the initial vibrational excitation energy. The open points in Figure 4 show the transient absorption in $CDCl_3$ of *cis*-stilbene and the solid points show it for *trans*-stilbene following the excitation of the stretch−bend combination band near 4800 cm^{-1}. The low energy of the excitation pulse makes the signal noisier, but the decay times that we obtain for the combination band are nearly the same as those of the overtone. The ratio of amplitudes of the two components (A_1/A_2) for the combination band excitation is about 30% larger in both isomers although the quality of the data produces large uncertainties.

IV. Discussion

Our measurements show that there are multiple time scales to the transient electronic absorption in both *cis*- and *trans*-stilbene and that they do not change significantly with solvent ($CDCl_3$, $(CD_3)_2CO$, or CD_3CN) or with vibrational excitation level, $2\nu_{CH}$ (5990 cm^{-1}) and $\nu_{CH} + \nu_{bend}$ (4650 cm^{-1}). Both of these observations help identify pathways and mechanisms of the vibrational energy flow.

A. Pathways. The similarity of the decay times in different solvents suggests that interactions within the vibrationally excited stilbene *primarily* control the relaxation that we observe and that our measurement is not sensitive to the flow of vibrational energy into the solvent. Even in the case of transfer between modes that lie close in energy within a solute molecule, the solvent potentially participates by making up small energy differences or bringing the levels into resonance, a crucial distinction between intramolecular energy flow for an isolated molecule and for a molecule in solution.[23] The influence on solvent is usually less dramatic when the energy flows within the solute (IVR) than when it flows into the solvent (IET), in agreement with the qualitative idea that solvent plays a more direct role as the recipient of energy in IET. For example, we have monitored the role of solvent in the vibrational relaxation of iodomethanes (CH_3I and CH_2I_2) after the excitation of the first overtone of the C−H stretch.[5,7] The rates of both IVR and IET depend on the identity of the solvent, but strongly interacting solvents have a larger effect on the rates of IET. They are *much* faster in the strongly interacting solvents C_6D_6 and $(CD_3)_2CO$ than in the weakly interacting solvents CCl_4 or $CDCl_3$,[4−6,24] increasing by a factor of more than three while the IVR rates grow by about 50% between weakly and strongly interacting solvents. Similarly, measurements on larger organic molecules, such as anthracene,[25] find no influence of the identity of the solvent on vibrational lifetimes. In general, solvent seems to have relatively little influence on the IVR at state densities above about 10 states/cm^{-1}. (The influence of solvent interaction on the IVR rate is greater for some molecules excited in the fundamental region, probably reflecting the ability of solvent to change couplings in these regions of sparse state density.[4,7])

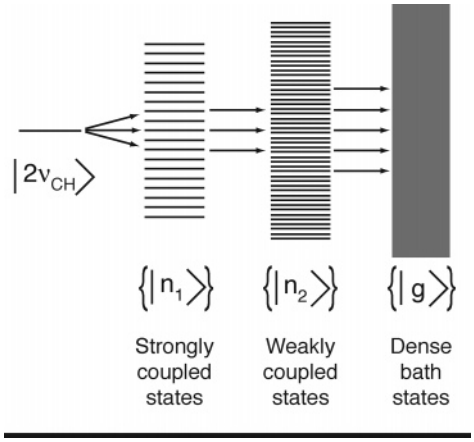

Figure 5. Schematic tier model of the states observed in transient absorption. The initial excitation prepares the nonstationary state $|2\nu_{CH}\rangle$, and energy flows sequentially through an intermediate sets of states, $\{|n_1\rangle\}$ and $\{|n_2\rangle\}$, and then into a set of final states, $\{|g\rangle\}$. The transient absorption probes the various tiers with different efficiency depending on their Franck−Condon factors.

Our detection method relies on population in the Franck−Condon active modes, limiting our observation to the flow of energy through these modes. Resonance Raman scattering shows that many of the Franck−Condon active modes of *cis*- and *trans*-stilbene[26−29] are nearly the same in the range of 900 to 1700 cm^{-1}, probably reflecting their common structures and suggesting that our experiments probe similar ring stretching and bending vibrations in both isomers. However, at wavenumbers below 900 cm^{-1}, *trans*-stilbene has one unique ring-breathing mode at 865 cm^{-1}, and *cis*-stilbene has two unique ring-torsion modes at 560 and 403 cm^{-1}. The differences in the decays and the sensitivity to the pathways in our data clearly depend on exactly which modes we probe, but single wavelength transient absorption does not allow us to distinguish among the Franck−Condon active modes.

B. Mechanism. The coupling of vibrational states is the controlling aspect of vibrational energy flow because the number of states available to accept energy initially deposited in one (nonstationary) state along with the coupling strengths determines the relaxation rate. Although each pair of states has its own unique coupling, a useful picture approximates the full complexity of the couplings as a series of tiers, illustrated in Figure 5, in which each successive tier contains states with roughly the same coupling strength to those in the adjacent tier. The initially populated state in most of our experiments is two quanta of C−H stretch ($|2\nu_{CH}\rangle$), and the next tier ($\{|n_1\rangle\}$) contains relatively strongly coupled states. In this model, the states in the next more weakly coupled tier ($\{|n_2\rangle\}$) interact with those in the previous tier roughly equally and couple to the initial state only through the intervening tier. For example, a member of the set $\{|n_1\rangle\}$ might be a state having one quantum of C−H stretching vibration replaced by two quanta of a lower frequency vibration. The order of the coupling between two states, the total number of quanta lost from the initial state and gained in the coupled state, is three in this example. Lower order couplings, corresponding to the exchange of fewer quanta, are usually stronger than higher order couplings.[30,31] Thus, higher frequency modes, which couple to the initially excited C−H stretch strongly through the exchange of only a few quanta, generally make up the first tier, and lower frequency modes, which couple by the exchange of more quanta, appear in other tiers of weakly coupled states. The slower decays in *cis*-stilbene may reflect different coupling strengths for some of the Franck−Condon active modes in the two molecules, effectively moving states from the strongly coupled tier to the weakly coupled tier and, hence, reducing the energy-transfer rate.

A tier model is a convenient means of considering coupling short of the statistical limit. In a sequential picture, vibrational energy quickly flows into the first tier of strongly coupled states and then flows through the rest of the molecule by passing through sequential tiers and, in solution, into the solvent. The sequential coupling through tiers is a useful picture that has grown out of frequency domain spectroscopy.[32] Several recent experiments provide time-domain evidence for this sequential relaxation and probe the role that solvent plays by comparing the evolution of state populations in isolated molecules and in solution. For example, measurements on the vibrational relaxation dynamics of CH_3I in the gas phase and in solution[24] using transient ultraviolet absorption show that vibrational energy only partially equilibrates within the molecule in solution, transferring energy only into a relatively strongly coupled subset of states before it dissipates into the surroundings. The critical observation is that the population of the vibrational states probed by transient electronic absorption evolves with two characteristic times in the gas phase. The initial fast relaxation (into the strongly coupled states) occurs in about 7 ps, and the subsequent slow relaxation (into the more weakly coupled states) in the isolated molecule takes about 400 ps. One cannot observe the slower relaxation in solution because energy flows into the solvent within 16 to 50 ps, long before it can sample the weakly coupled states.[24]

A simple interpretation in terms of the strongly and weakly coupled tiers explains the observation in CH_3I and in several other molecules. Abel and co-workers also used transient electronic absorption to monitor two times scales for energy flow in isolated benzene,[33,34] and Pate and co-workers have observed multiple time scales (and recurrences) using transient IR absorption.[23,35,36] Recent experiments by Yamada et al.[37] directly probe the tiers in isolated phenol where energy initially deposited in an O−H stretch state flows into the "doorway state(s)" before dissipating into the dense bath states. Following the relaxation of a fundamental O−H stretch, they find that a two-step tier model explains their results where the first tier contains specific doorway states strongly coupled to the O−H stretch in phenol and the second tier contains the dense bath states.

The two decays we observe in stilbene probably reflect a similar sequential energy flow through sets of states. Figure 5 summarizes the likely relaxation mechanism in *cis*- and *trans*-stilbene. After fast relaxation from the initially excited state ($\tau_1 \sim 1$ ps), energy flows more slowly through the tiers ($\{|n_1\rangle\}$ and $\{|n_2\rangle\}$) producing the slower components (τ_2 and τ_3). The signal grows with transfer into the more strongly coupled states (which have many of the Franck−Condon active modes) and subsequently decays as energy flows into the denser manifold of more weakly coupled states (which have fewer Franck−Condon active modes) before flowing out of the molecule into the solvent. Because our ability to distinguish the flow among the tiers rests on their having different efficiencies in the probe step, some of the relatively high-frequency Franck−Condon active modes in the range of 900 to 1700 cm^{-1} are good candidates for the first tier ($\{|n_1\rangle\}$) and the lower frequency Franck−Condon active modes are the most suitable for the next tier ($\{|n_2\rangle\}$).

The 2-fold difference in decay times for *trans*-stilbene and *cis*-stilbene apparently reflects the different couplings among the states in the molecules. Slight changes in energies of the

modes may move their positions relative to the initially excited C−H stretch, changing the effective coupling and, hence, the rate of energy flow. The initial decays of $\tau_2^{cis} = 2.6$ ps for *cis*-stilbene and $\tau_2^{trans} = 1.4$ ps for *trans*-stilbene are consistent with a strong, low-order coupling between the C−H stretch overtone and nearby states, and the slower decays of $\tau_3^{cis} = 24$ ps for *cis*-stilbene and $\tau_3^{trans} = 10$ ps for *trans*-stilbene are on the order of times we have observed for relaxation into a denser tier of more weakly coupled states.[5,7] The insensitivity of the decay times to the excitation level is consistent with the participation of only a subset of all of the states in the molecule in the relaxation observed through the window of the Franck−Condon active modes.

The total vibrational state density increases rapidly with increasing energy, but most of these additional modes contain many quanta of low-frequency excitation and are, thus, weakly coupled to the initially excited state. By contrast, the state structure of the strongly coupled, high-frequency modes changes little with excitation level.[7] It is likely that the two decays we observe in stilbene reflect the passage of energy sequentially through states with different efficiencies and that the change in the relative amplitudes of the decay components comes from differences in the composition of weakly coupled tiers.

V. Summary

We have used IR excitation of either the first C−H stretch overtone ($2\nu_{CH}$) or the stretch−bend combination ($\nu_{CH} + \nu_{bend}$) to prepare vibrations in both the *cis*- and *trans*-isomers of stilbene and have monitored the subsequent flow of energy in the excited molecule using transient electronic absorption. Both isomers have two distinct decay times following the initial rise of the signal as energy flows out of the initially excited state into ones that have good Franck−Condon factors for the probe transition. The decay times are about a factor of 2 longer in *cis*-stilbene ($\tau_2^{cis} = (2.6 \pm 1.5)$ ps and $\tau_3^{cis} = (24.1 \pm 2.1)$ ps) than in *trans*-stilbene ($\tau_2^{trans} = (1.4 \pm 0.6)$ ps and $\tau_3^{trans} = (10.2 \pm 1.1)$ ps), but they do not change with either the interaction strength of the solvent or the vibrational excitation energy. The lack of a dependence of the relaxation time on solvent interaction suggests that the flow of energy that we observe is primarily intramolecular (IVR), occurring *within* the initially excited molecule. The indifference to the initial vibrational energy indicates that coupling among a subset of states, whose structure is similar at the two vibrational excitation levels, controls the energy flow among the states we observe. Both of these behaviors are consistent with the tier model of energy flow, shown in Figure 5, in which the initial excitation migrates through tiers of energy levels that we probe with different efficiencies because their average Franck−Condon factors are different. The factor of 2 difference in the decay times between *cis*-stilbene and *trans*-stilbene seems to reflect the coupling strengths for some of the Franck−Condon active modes in the two molecules. Within each molecule, the structure of the few tiers we observe is probably similar at the two excitation energies of the measurements, and the relatively strong coupling is not very sensitive to solvent interactions, as we have observed in other cases.

Acknowledgment. We thank G. L. Barnes for help with some of the measurements, Dr. C. G. Elles for several useful discussions, and L. Sheps for a careful reading of the manuscript and helpful suggestions. We gratefully acknowledge the support of this work by the Air Force Office of Scientific Research.

References and Notes

(1) Oxtoby, D. W. *Adv. Chem. Phys.* **1981**, *47*, 487.
(2) Owrutsky, J. C.; Ragtery, D.; Hochstrasser, R. M. *Annu. Rev. Phys. Chem.* **1994**, *45*, 519.
(3) Elsaesser, T.; Kaiser, W. *Annu. Rev. Phys. Chem.* **1991**, *42*, 83.
(4) Heckscher, M. M.; Sheps, L.; Bingemann, D.; Crim, F. F. *J. Chem. Phys.* **2002**, *117*, 8917.
(5) Bingemann, D.; King, A. M.; Crim, F. F. *J. Chem. Phys.* **2000**, *113*, 5018.
(6) Cheatum, C. M.; Heckscher, M. M.; Bingemann, D.; Crim, F. F. *J. Chem. Phys.* **2001**, *115*, 7086.
(7) Elles, C. G.; Bingemann, D.; Heckscher, M. M.; Crim, F. F. *J. Chem. Phys.* **2003**, *118*, 5587.
(8) Charvat, A.; Assmann, J.; Abel, B.; Schwarzer, D.; Henning, K.; Luther, K.; Troe, J. *Phys. Chem. Chem.* Phys. **2001**, *3*, 2230.
(9) Charvat, A.; Assmann, J.; Abel, B.; Schwarzer, D. *J. Phys. Chem. A* **2001**, *105*, 5071.
(10) McIlroy, A.; Nesbitt, D. J. *J. Chem. Phys.* **1990**, *92*, 2229.
(11) McWhorter, D. A.; Pate, B. H. *J. Phys. Chem. A* **1998**, *102*, 8786.
(12) Wilhelm, T.; Piel, J.; Riedle, E. *Opt. Lett.* **1997**, *22*, 1494.
(13) Shirakawa, A.; Sakane, I.; Kobayashi, T. *Opt. Lett.* **1998**, *23*, 1292.
(14) Danielius, R.; Piskarskas, A.; DiTrapani, P.; Andreoni, A.; Solcia, C.; Foggi, P. *Opt. Lett.* **1996**, *21*, 973.
(15) Choi, C. H.; Kertesz, M. *J. Phys. Chem. A* **1997**, *101*, 3823.
(16) Sension, R. J.; Repinec, S. T.; Szarka, A. Z.; Hochstrasser, R. M. *J. Chem. Phys.* **1993**, *98*, 6291.
(17) Sension, R. J.; Szarka, A. Z.; Hochstrasser, R. M. *J. Chem. Phys.* **1992**, *97*, 5239.
(18) Nikowa, L.; Schwarzer, D.; Troe, J. *Chem. Phys. Lett.* **1995**, *233*, 303.
(19) Nakabayashi, T.; Okamoto, H.; Tasumi, M. *J. Phys. Chem. A* **1998**, *102*, 9686.
(20) Nakabayashi, T.; Okamoto, H.; Tasumi, M. *J. Phys. Chem. A* **1997**, *101*, 7189.
(21) Qian, J.; Schultz, S. L.; Jean, J. M. *Chem. Phys. Lett.* **1995**, *233*, 9.
(22) Miller, K. J. *J. Am. Chem. Soc.* **1990**, *112*, 8533.
(23) Yoo, H. S.; DeWitt, M. J.; Pate, B. H. *J. Phys. Chem. A* **2004**, *108*, 1348.
(24) Elles, C. G.; Cox, M. J.; Crim, F. F. *J. Chem. Phys.* **2004**, *120*, 6973.
(25) Emmerling, F.; Lettenberger, M.; Laubereau, A. *J. Phys. Chem.* **1996**, *100*, 19251.
(26) Myers, A. B.; Mathies, R. A. *J. Chem. Phys.* **1984**, *81*, 1552.
(27) Myers, A. B.; Trulson, M. O.; Mathies, R. A. *J. Chem. Phys.* **1985**, *83*, 5000.
(28) Hamaguchi, H.; Kato, C.; Tasumi, M. *Chem. Phys. Lett.* **1983**, *100*, 3.
(29) Hamaguchi, H.; Urano, T.; Tasumi, M. *Chem. Phys. Lett.* **1984**, *106*, 153.
(30) Gruebele, M.; Bigwood, R. *Int. Rev. Phys. Chem.* **1998**, *17*, 91.
(31) Gruebele, M.; Wolynes, P. G. *Acc. Chem. Res.* **2004**, *37*, 261.
(32) Nesbitt, D. J.; Field, R. W. *J. Phys. Chem.* **1996**, *100*, 12735.
(33) Assmann, J.; von Benton, R.; Charvat, A.; Abel, B. *J. Phys. Chem. A* **2003**, *107*, 1904.
(34) von Benten, R.; Link, O.; Abel, B.; Schwarzer, D. *J. Phys. Chem. A* **2004**, *108*, 363.
(35) Yoo, H. S.; DeWitt, M. J.; Pate, B. H. *J. Phys. Chem. A* **2004**, *108*, 1365.
(36) Yoo, H. S.; McWhorter, D. A.; Pate, B. H. *J. Phys. Chem. A* **2004**, *108*, 1380.
(37) Yamada, Y.; Mikami, N.; Ebata, T. *J. Chem. Phys.* **2004**, *121*, 11530.